J Indian Soc Remote Sens
DOI 10.1007/s12524-017-0698-2

RESEARCH ARTICLE

Examining the Effect of Ancillary and Derived Geographical Data on Improvement of Per-Pixel Classification Accuracy of Different Landscapes

Uttam Kumar[1,5] · Anindita Dasgupta[1] · Chiranjit Mukhopadhyay[2] · T. V. Ramachandra[1,3,4]

Received: 10 August 2016 / Accepted: 8 June 2017
© Indian Society of Remote Sensing 2017

Abstract Effective conservation and management of natural resources requires up-to-date information of the land cover (LC) types and their dynamics. Multi-resolution remote sensing (RS) data coupled with additional ancillary topographical layers (both remotely acquired or derived from ground measurements) with appropriate classification strategies would be more effective in capturing LC dynamics and changes associated with the natural resources. Ancillary information would make the decision boundaries between the LC classes more widely separable, enabling classification with higher accuracy compared to conventional methods of RS data classification. In this work, we ascertain the possibility of improvement in classification accuracy of RS data with the addition of ancillary and derived geographical layers such as vegetation indices, temperature, digital elevation model, aspect, slope and texture, implemented in three different terrains of varying topography—urbanised landscape (Greater Bangalore), forested landscape (Western Ghats) and rugged terrain (Western Himalaya). The study showed that use of additional spatial ancillary and derived information significantly improved the classification accuracy compared to the classification of only original spectral bands. The analysis revealed that in a highly urbanised area with less vegetation cover and contrasting features, inclusion of elevation and texture increased the overall accuracy of IKONOS data classification to 88.72% (3.5% improvement), and inclusion of temperature, NDVI, EVI, elevation, slope, aspect, Panchromatic band along with texture measures, significantly increased the overall accuracy of Landsat ETM+ data classification to 83.15% (7.6% improvement). In a forested landscape with moderate elevation, temperature was useful in improving the overall accuracy by 6.7 to 88.26%, and in a rugged terrain with temperate climate, temperature, EVI, elevation, slope, aspect and Panchromatic band significantly improved the classification accuracy to 89.97% (10.84% improvement) compared to the classification of only original spectral bands, suggesting selection of appropriate ancillary data depending on the terrain.

Keywords Land cover · Classification · Accuracy · Ancillary layers · DEM · Vegetation indices · Texture

✉ T. V. Ramachandra
cestvr@ces.iisc.ernet.in;
http://ces.iisc.ernet.in/energy

[1] Energy & Wetlands Research Group [CES TE15], Centre for Ecological Sciences, Indian Institute of Science, Third Floor, E Wing, New Bioscience Building [Near D Gate], Bangalore, Karnataka 560012, India

[2] Department of Management Studies, Indian Institute of Science, Bangalore, Karnataka 560 012, India

[3] Centre for Sustainable Technologies (Astra), Indian Institute of Science, Bangalore, Karnataka 560 012, India

[4] Centre for Infrastructure, Sustainable Transportation and Urban Planning (CiSTUP), Indian Institute of Science, Bangalore, Karnataka 560 012, India

[5] NASA Ames Research Center, Moffett Field, Mountain View, CA 94035, USA

Introduction

Classification of remote sensing (RS) data accurately is a requirement for many applications such as global change research (Nemani et al. 2011), geological research (Smith et al. 1985), wetlands mapping (Ramachandra and Kumar 2008), crop estimation (Pacheco and McNairn 2010), vegetation classification (Hostert et al. 2003), forest

Published online: 04 July 2017

classification (Huang et al. 2008), urban studies (Pu et al. 2008), feature extraction (Dópido et al. 2011), land cover (LC) change (Turner et al. 1994), Earth system modelling (Collins et al. 2011), etc. Satisfactory classification of RS data depends on many factors including (a) the characteristics of study area, (b) availability of suitable RS data, (c) ancillary and ground reference data, (d) proper use of variables and classification algorithms, (e) user's experience with reference to the application and (f) time constraints (Lu and Weng 2005). Furthermore, diverse landscapes and terrain types have a mixture of both homogeneous and heterogeneous LC classes and require supplemental environmental or geographical layers for improved classification accuracies. Increased spectral variation is common with high degree of spectral heterogeneity; for example, urban landscapes are composed of features having a complex mix of buildings, roads, trees, lakes, lawns, concrete, etc., often responsible for low classification accuracy. In landscapes with mountains and dense forests, problems arise due to changes in elevation, topographic differences and often shades (shadows) produced by hillocks and long trees due to altitudinal variations, which is a major challenge for selection of suitable image processing approach. Fine spatial resolution data such as IKONOS Multispectral (MS) and Panchromatic (PAN) often lead to high spectral variation within the same LC class resulting in poor classification performance (Lu et al. 2010). Therefore, reducing the spectral variation within the same LC and increasing the separability of different LC types are the keys for improving LC classification (Lu and Weng 2007). In practice, data acquired from medium spatial resolution sensors such as Landsat TM/ETM+ or IRS LISS-III, being readily available for multiple dates, are commonly used for most landscape analysis (urban and forested terrain at a regional scale). In this regard, different approaches such as multi-sensor data integration (Haack et al. 2002), full spectral image classification (Stuckens et al. 2000; Shaban and Dikshit 2001), expert classification (Hung and Ridd 2002), etc. have been used. Traditional per-pixel spectral-based supervised classification is based only on spectral signatures, and does not make use of rich spatial information inherent in the data (Lu et al. 2010). Therefore, making full use of RS information along with ancillary information (acquired or derived environmental layers) would be an efficient way to improve classification accuracy. For example, Na et al. (2010) used 103 geographical layers to show improvement in LC mapping using Landsat TM bands 1–5 and 7, NDVI (Normalised Difference Vegetation Index), EVI (Enhanced Vegetation Index), a data fusion transformation combining the six bands information from the Landsat TM image (first principal component—PC1) as additional predictors, image texture measures (variance, homogeneity, contrast, dissimilarity and entropy) with window size of 3×3 pixels and 11×11 pixels, DEM, slope and soil type with Random Forest (RF), Classification and Regression Tree (CART) and Maximum Likelihood Classifier (MLC) based classification. Among these, RF yielded accurate classification with an overall accuracy of 91% and kappa 0.8943. They also quantified the effect of training set size on the performance of classification algorithms. Xiaodong et al. (2009) integrated TM data with NDVI, EVI, PC1, slope, soil types and five texture measures (variance, homogeneity, contrast, dissimilarity and entropy) for LC classification of Marsh Area using Classification Trees and MLC. They concluded that image spectral, textural, terrain data and ancillary Geographical Information System (GIS) improved the land use land cover (LULC) classification accuracy significantly. Fahsi et al. (2000) evaluated the contribution and quantified the effectiveness of DEM (digital elevation model) in improving LC classification using Landsat TM data over a rugged area in the Atlas Mountains, Morocco which considerably improved the classification accuracy by reducing the effect of relief on satellite images, increasing the individual accuracies of the different classes by up to 60%. Recio et al. (2011) used historical land use (LU) and ancillary data and showed improvement in overall classification accuracy considered case-by-case for each class. Masocha and Skidmore (2011) used DEM along with ASTER imagery and georeferenced point data obtained from field to increase the accuracy of invasive species (Lantana camera) mapping using Neural Network and SVM (support vector machine) hybrid classifiers. The overall accuracy increased from 71% (kappa 0.61) to 83% (kappa 0.77) with Neural Network and from 64% (kappa 0.52) to 76% (kappa 0.67) with SVM hybrid classifiers. Dorren et al. (2003) studied the effect of topographic correction and the role of DEM as additional band using per-pixel and object based classification to classify forest stand type maps using Landsat TM data in a steep mountainous terrain. They concluded that both topographic correction and classification with DEM as additional band increased the overall accuracy. Xian et al. (2008) quantified multi-temporal urban development characteristics in Las Vegas from Landsat and ASTER Data. Apart from the satellite imageries, NDVI, slope, aspect and temperature were used for classification. Lu and Weng (2005) demonstrated urban classification using full spectral information of Landsat ETM+ imagery in Marion County, Indiana using PC's of ETM+ MS bands, texture, temperature and data fusion of MS and PAN. They concluded that texture and temperature may improve classification accuracy for some classes, but may degrade for other classes. Data fusion of MS and PAN are useful but high spatial resolution also increases spectral variation within the classes, decreasing the classification accuracy. Data fusion

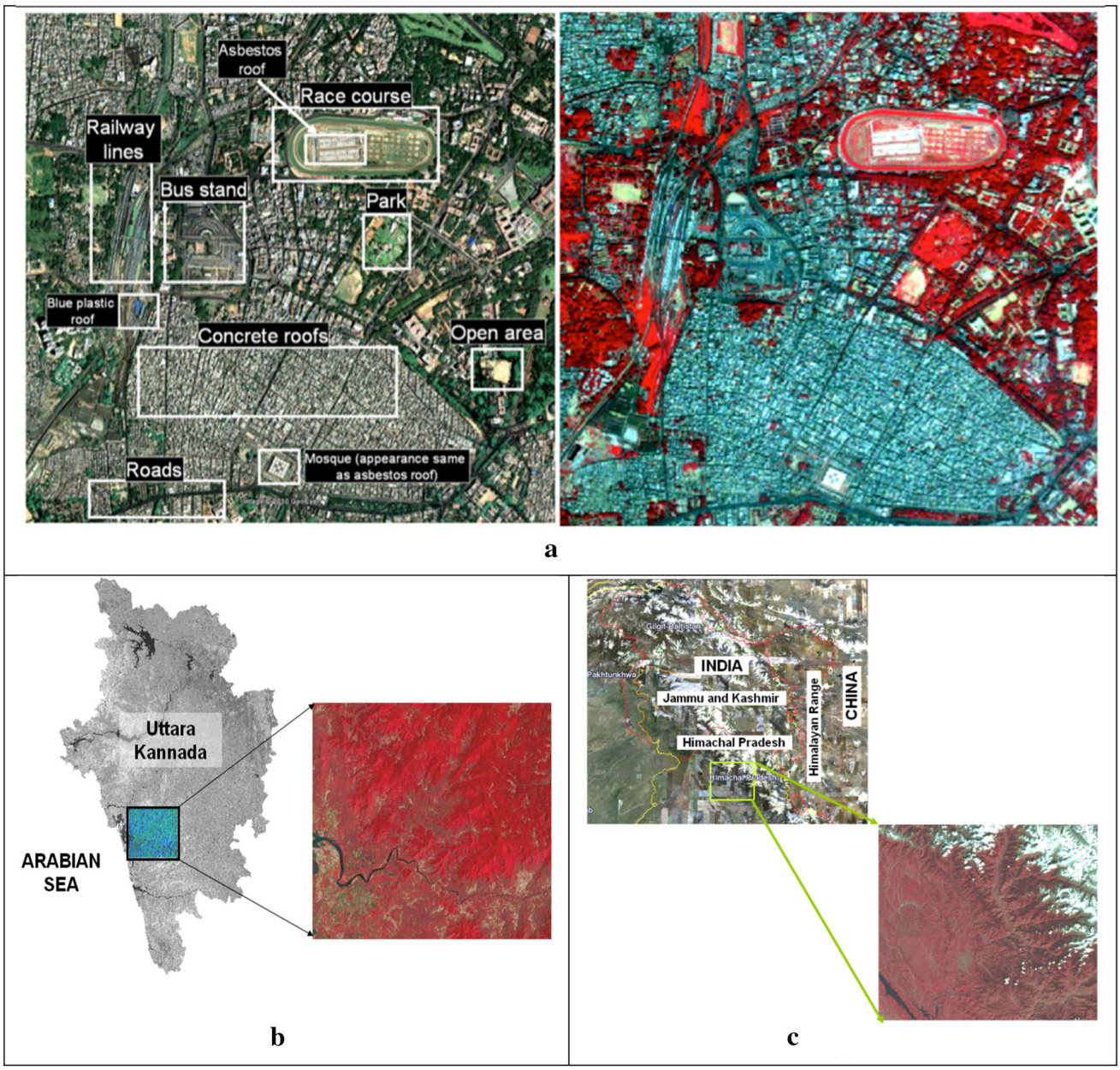

Fig. 1 **a** Part of greater Bangalore City as seen in Google Earth (*left*) and IKONOS image (*right*); **b** location of the study area in Central Western Ghats; and **c** location of study area in Western Himalaya (colour figure online)

combined with texture significantly improves classification accuracy.

In this study, three different terrain types with varying characteristics in the Indian context are considered for classification with Landsat ETM+ MS bands and several other ancillary and derived layers using Random Forest (RF) classifier. The role of vegetation indices such as NDVI and EVI, elevation and derived layers (slope and aspect), temperature, texture (Haralick et al. 1973; Haralick 1979; GRASS GIS 2017), and addition of PAN band in addition to MS bands are examined in the process of image classification.

Study Area and Data

Urban Classification: Greater Bangalore

The study area selected for urban classification is a part of the city of Greater Bangalore as seen in Google Earth image in Fig. 1a). The area in the scene is highly urbanised with the central business district. It consists of highly contrasting and heterogeneous features—race course (as oval shape in the first quadrant of the image), bus stand with semi-circular platforms, railway station with railway lines in the second quadrant, a park below the race course,

Table 1 Details of geographical layers used for IKONOS data classification

Classification No.	RS data and ancillary layers	Total number of input layers
1	IKONOS bands 1, 2, 3, 4	4
2	IKONOS bands 1, 2, 3, 4 and NDVI	5
3	IKONOS bands 1, 2, 3, 4 and EVI	5
4	IKONOS bands 1, 2, 3, 4 and DEM	5
5	IKONOS bands 1, 2, 3, 4, EVI, DEM	6
6	IKONOS bands 1, 2, 3, 4, DEM, slope and aspect	7
7	IKONOS bands 1, 2, 3, 4, DEM, slope, aspect and EVI	8
8	IKONOS bands 1, 2, 3, 4, DEM and Texture (ASM, contrast, entropy, variance) at 0, 45, 90 and 135 degrees for IKONOS bands 1, 2, 3, 4	$5 + (4 \times 4 \times 4) = 69$

Table 2 Details of data and ancillary layers for Landsat ETM+ MS classification of Bangalore City

Classification No.	RS data and ancillary layers	Total number of input layers
1	ETM+ bands 1, 2, 3, 4, 5 and 7 at 30 m	6
2	ETM+ bands 1, 2, 3, 4, 5, 7 and Temperature	7
3	ETM+ bands 1, 2, 3, 4, 5, 7, NDVI, EVI, elevation, slope and aspect	11
4	ETM+ bands 1, 2, 3, 4, 5, 7, Temperature, NDVI, EVI, elevation, slope and aspect	12
5	ETM+ bands 1, 2, 3, 4, 5, 7, Temperature, NDVI, EVI, elevation, slope and aspect, texture (ASM, contrast, entropy, variance) at 0, 45, 90 and 135 degrees for ETM+ bands 1, 2, 3, 4, 5, 7	108
6	ETM+ bands 1, 2, 3, 4, 5, 7, Temperature, NDVI, EVI, elevation, slope and aspect, texture (ASM, contrast, entropy, variance) at 0, 45, 90 and 135 degrees for ETM+ bands 1, 2, 3, 4, 5, 7	109
7	ETM+ bands 1, 2, 3, 4, 5, 7, Temperature, NDVI, EVI, elevation, slope and aspect, ETM+ PAN, texture (ASM, contrast, entropy, variance) at 0, 45, 90 and 135 degrees for ETM+ bands 1, 2, 3, 4, 5, 7, and ETM+ PAN	125

Table 3 Details of data and ancillary layers for Landsat ETM+ MS classification for a part of Central Western Ghats

Classification No.	RS data and ancillary layers	Total number of input layers
1	ETM+ bands 1, 2, 3, 4, 5 and 7 at 30 m	6
2	ETM+ bands 1, 2, 3, 4, 5, 7 and Temperature	7
3	ETM+ bands 1, 2, 3, 4, 5, 7, elevation	7
4	ETM+ bands 1, 2, 3, 4, 5, 7, EVI	7
5	ETM+ bands 1, 2, 3, 4, 5, 7, elevation, slope and aspect	9
6	ETM+ bands 1, 2, 3, 4, 5, 7, Temperature, EVI, PAN	9
7	ETM+ bands 1, 2, 3, 4, 5, 7, Temperature, EVI, PAN, texture (contrast, variance) at 0, 45, 90 and 135 degrees for ETM+ bands 1, 2, 3, 4, 5, 7, and ETM+ PAN	65

dense builtup with concrete roofs, and some buildings with asbestos roofs, blue plastic roofs (one in the vicinity of the race course and 2 near the railway lines), tarred roads with flyovers, vegetation and few open areas (such as play ground, walk ways and vacant land). Dense and medium urban areas have high surrounding temperature compared to vegetation patches, parks and lakes (Ramachandra and Kumar 2009). The undulating terrain in the city ranges from 735 to 970 m with varying textures due to different urban structures. For this terrain two different data sets were used for the demonstration of urban classification—IKONOS MS and Landsat ETM+ MS.

IKONOS data along with ancillary and derived layers such as elevation, slope, NDVI, EVI and textures (ASM—angular second moment, contrast, entropy and variance) were used in separate experiments during classification as summarised in Table 1. In another set of experiments, Landsat ETM+ data with 6 MS bands (resampled to 15 m)

Table 4 Details of data and ancillary layers for Landsat ETM+ MS classification in Western Himalaya

Classification No.	RS data and ancillary layers	Total number of input layers
1	ETM+ bands 1, 2, 3, 4, 5 and 7 at 30 m	6
2	ETM+ bands 1, 2, 3, 4, 5, 7 and Temperature	7
3	ETM+ bands 1, 2, 3, 4, 5, 7, elevation	7
4	ETM+ bands 1, 2, 3, 4, 5, 7, EVI	7
5	ETM+ bands 1, 2, 3, 4, 5, 7, elevation, slope and aspect	9
6	ETM+ bands 1, 2, 3, 4, 5, 7, Temperature, EVI, elevation, slope and aspect	11
7	ETM+ bands 1, 2, 3, 4, 5, 7, Temperature, EVI, elevation, slope, aspect and ETM+ PAN	12
8	ETM+ bands 1, 2, 3, 4, 5, 7, Temperature, EVI, texture (ASM, contrast, entropy, variance) at 0, 45, 90 and 135 degrees for ETM+ bands 1, 2, 3, 4, 5, 7	104
9	ETM+ bands 1, 2, 3, 4, 5, 7 and texture (ASM, contrast, entropy, variance) at 0, 45, 90 and 135 degrees for ETM+ bands 1, 2, 3, 4, 5, 7	102

along with geographical layers, PAN and texture measures from PAN band making the total number of geographical layers to 125, were used in the classification as summarised in Table 2.

Forested Landscape with Undulating Terrain: Case Study of Uttara Kannada District, Central Western Ghats

This region has gentle undulating hills, rising steeply from a narrow coastal strip bordering the Arabian sea to a plateau at an altitude of 500 m with occasional hills rising above 600–860 m. Climatic conditions range from arid to humid due to physiographic conditions ranging from plains, mountains to coast. Seven classifications were carried out with different combinations of Landsat ETM+ bands and geographical layers (such as temperature, elevation, EVI, slope, aspect, PAN and texture i.e. contrast and variance as listed in Table 3) into agriculture, builtup, forest, plantation, wasteland and water bodies that are the six major land use categories in the forested and mountainous terrain of Uttara Kannada district (Fig. 1b). The total number of geographical layers were altogether 65 as shown in Classification No. 7 in Table 3 which included Landsat ETM+ bands 1–5 and 7, temperature, EVI, PAN and texture (contrast and variance computed at 0, 45, 90 and 135 degrees on ETM+ bands 1–5, 7 and ETM+ PAN band).

Mountainous Terrain in Temperate Climate: Mandhala Watershed, Western Himalaya

Mandhala watershed falls in lower Shivalik range of the Himalayas (Fig. 1c), dominated by dry evergreen tree species. This region is characterised by rugged terrain of Western Himalaya with altitude ranging from 295 to 6619 m above mean sea level. Nine different classification with combinations of Landsat ETM+ spectral bands, PAN and ancillary layers (viz. temperature, elevation, EVI, slope, aspect and texture) were carried out into four categories—vegetation, water, snow and others (settlement, rock, barren). In Classification No. 8, the combination of Landsat ETM+ bands, temperature, EVI and texture produced the highest number of input layers i.e. 104 (Table 4). Finally in Classification No. 9, only original spectral bands and their texture measures were considered (temperature and EVI layers were ignored) to make the total number of input layers in classification to 102 as seen in Table 4. It is to be noted that high spatial resolution IKONOS data were not available for forested landscape in Western Ghats and for the Himalayan terrain.

The classifications were performed using RF which uses bagging to form an ensemble of classification tree. At each splitting node in the underlying classification trees, a random subset of the predictor variables is used as potential variables to define split. In training, it creates multiple Classification and Regression Tree trained on a bootstrapped sample of the original training data, and searches only across randomly selected subset of the input variables to determine a split for each node. The output of the classifier is determined by a majority vote of the trees that result in the greatest classification accuracy. It is superior to many tree-based algorithms, because it lacks sensitivity to noise and does not overfit. The trees in RF are not pruned; therefore, the computational complexity is reduced. As a result, RF can handle high dimensional data, using a large number of trees in the ensemble (Breiman and Cutler 2010). All the experiments were carried out on a Desktop computer with Intel Pentium IV processor, 3.00 GHz clock speed and 3.5 Gb RAM in Linux with GRASS GIS and R statistical package.

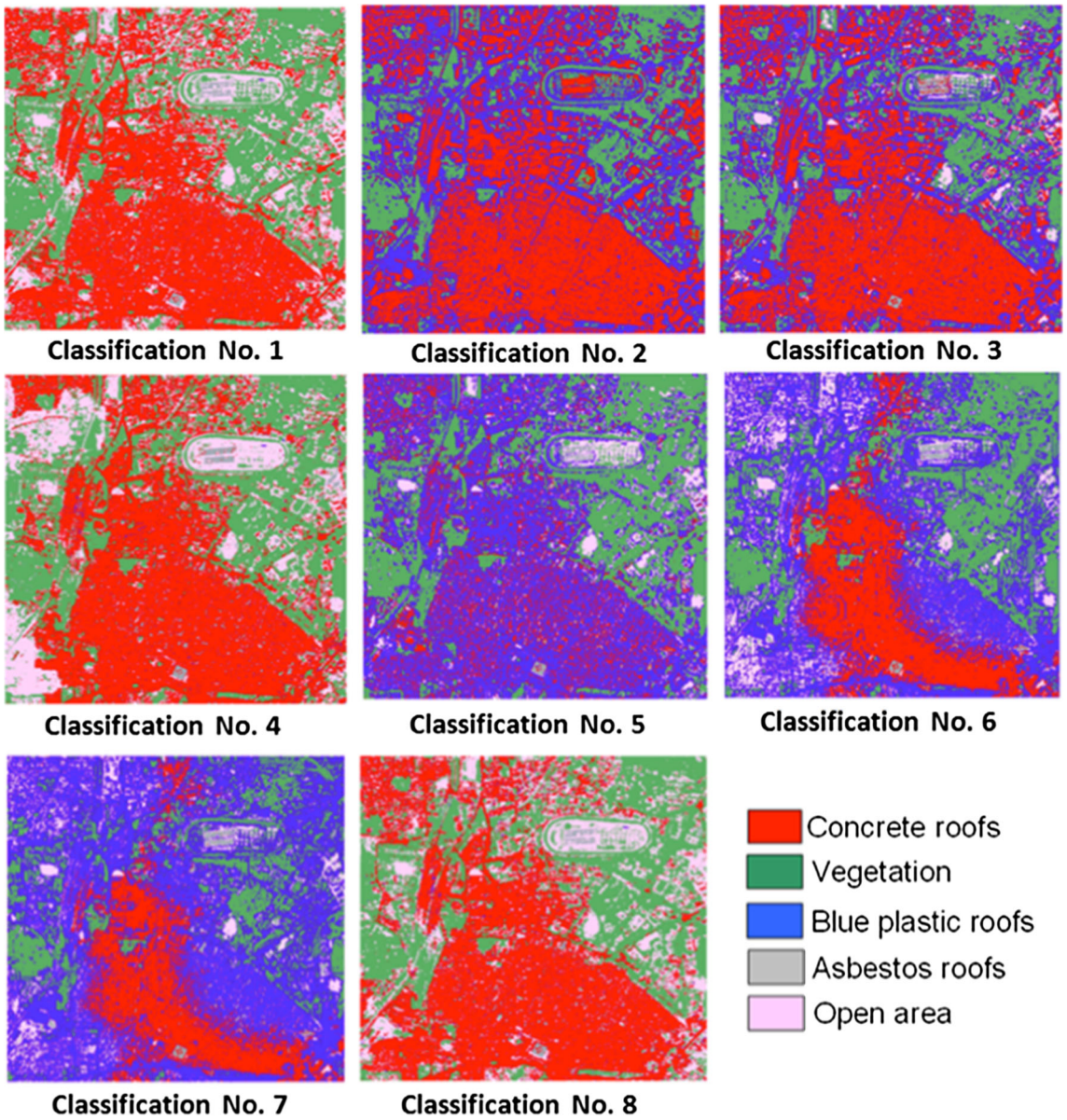

Fig. 2 Classified outputs from IKONOS by adding additional geographical layers (colour figure online)

Results and Discussion

Urban classification using IKONOS MS bands

It was observed that EVI highlight non-woody vegetation better than NDVI where the elevation ranged from 883 to 940 m. Figure 2 is the output from the 8 classifications as explained in Table 5 using RF. Figure 2 (Classification No. 1) is the classified output of IKONOS 4 bands using RF. Classification No. 2 is the output after adding NDVI as an additional layer to the input in the classifier, where two classes are missing (asbestos roof and open area). Overall, blue plastic roof is over estimated (which is not a consequence of training error) as evident from Fig. 2 and area statistics in Table 5. The role of NDVI in discriminating non-vegetation area is negligible and therefore asbestos and open areas have merged with concrete roof and blue plastic with a drastic decrease in overall accuracy (47%) as shown in Table 6. When EVI was added as an additional derived layer, classification was better compared to the inclusion of NDVI. However, the class composition is either under estimated (concrete roof, vegetation and open area) or over estimated (blue plastic roof) lowering the overall accuracy to 55%. Blue plastic roof was also over estimated when both EVI and DEM were added as input layers along with the original bands. As evident from Fig. 2, concrete roof and open area have been misclassified and merged to blue plastic roof, which is dominant in the

Table 5 Area statistics obtained from the IKONOS classified images

Area		Class					
		Concrete roof	Asbestos roof	Blue plastic roof	Vegetation	Open area	Total
Classification No. 1	ha	**351.74**	**9.53**	**1.88**	**260**	**158.80**	781.76 ha
	%	**44.99**	**1.22**	**0.24**	**33.26**	**20.66**	(100%)
Classification No. 2	ha	324.51	–	285.02	172.23	–	
	%	41.51	–	36.46	22.03	–	
Classification No. 3	ha	299.89	7.26	259.32	188.17	27.11	
	%	38.36	0.93	33.17	24.07	3.47	
Classification No. 4	ha	**344.74**	**8.82**	**1.42**	**259.98**	**166.8**	
	%	**44.1**	**1.13**	**0.18**	**33.25**	**21.34**	
Classification No. 5	ha	84.53	11.20	385.11	244.86	56.06	
	%	10.81	1.43	49.26	31.32	7.17	
Classification No. 6	ha	142.56	17.44	331.30	218.02	72.44	
	%	18.24	2.23	42.38	27.89	9.27	
Classification No. 7	ha	126.17	16.13	433.22	146.88	59.36	
	%	16.14	2.06	55.42	18.79	7.59	
Classification No. 8	ha	**354.88**	**7.93**	**0.95**	**259.33**	**158.66**	
	%	**45.40**	**1.22**	**0.12**	**33.17**	**20.30**	

scene. Asbestos roof and vegetation are the two classes which showed higher producer's and user's accuracies. However, the overall accuracy still remained low (49.28%). Similar situation prevails when DEM, slope and aspect were included with the input IKONOS MS bands to the classifier. Concrete roof, open area and vegetation are under estimated and blue plastic roof is over estimated, bringing the overall accuracy to as low as 55%. The output worsens when DEM, slope, aspect with EVI were considered additionally to the input. All the classes are either over estimated or under estimated with overall accuracy of 51% (Table 6).

In classification No. 8, when only DEM and texture measures were added (Table 1) as input to the classifier apart from IKONOS 4 MS bands, the overall accuracy went high to 88.72% with high producer's and user's accuracies for individual classes which were classified properly (Table 5). The experiments conclude that in a highly urbanised area with less vegetation cover and highly contrasting features, texture plays a major role in discriminating individual classes which are rather difficult to distinguish using only original high spatial resolution IKONOS MS bands as evident from high classification accuracies in Table 6 and area statistics in Table 5 (Classification No. 4 and 8 highlighted in bold), compared to the classification of only IKONOS 4 MS bands (Classification No. 1 highlighted in bold). However, in Classification No. 4, concrete roof in top and bottom left areas of the image have been misclassified as open area as also evident from Table 5. DEM plays a role when the terrain is undulating but derived layers such as slope and aspect did not aid in discriminating classes when the elevation had low variance. Due to limited vegetation presence (a few parks) in the study area, EVI was not useful in classification. Overall 3.5% improvement in accuracy was observed after including elevation and texture along with the original bands as input to the classifier.

Urban Classification Using Landsat ETM+ Bands

Figure 3 shows output from the seven classified images and LU statistics are listed in Table 7. The producer's, user's, overall accuracies and kappa are given in Table 8. Figure 3 indicates that outputs obtained from the original spectral bands along with temperature, NDVI, EVI, elevation, slope and aspect (Classification No. 1, 2, 3 and 4) have misclassified many pixels belonging to builtup, water and open area. Many of the tarred or concrete road pixels that actually belong to builtup have been classified as water. Thus water class has been over estimated.

From accuracy assessment in Table 8, we see that Classification No. 5, 6 and 7 have higher accuracies compared to other classifications. Inclusion of temperature increased accuracy whereas addition of vegetation index layers along with elevation, slope and aspect decreased the overall accuracy. When both temperature and vegetation index with elevation, slope and aspect were used, the accuracy still decreased. However, inclusion of texture and

Table 6 Accuracy assessment of the IKONOS classified images

Accuracy	Class						
	Concrete roof	Asbestos roof	Blue plastic roof	Vegetation	Open area	OA (%)	Kappa
Classification No. 1							
PA (%)	**88.20**	**83.92**	**84.00**	**83.19**	**86.92**	**85.25**	**0.8250**
UA (%)	**88.99**	**81.00**	**87.00**	**82.77**	**88.00**		
Classification No. 2							
PA (%)	76.22	–	17.01	48.55	–	47.63	0.4136
UA (%)	69.45	–	21.97	51.33	–		
Classification No. 3							
PA (%)	83.77	91.34	10.55	48.00	18.00	55.05	0.5117
UA (%)	70.53	97.63	42.31	41.38	17.09		
Classification No. 4							
PA (%)	**84.15**	**89.48**	**88.53**	**85.07**	**82.18**	**85.88**	**0.8437**
UA (%)	**83.57**	**84.39**	**89.11**	**85.95**	**84.79**		
Classification No. 5							
PA (%)	42.89	73.94	10.05	78.53	55.91	49.28	0.4577
UA (%)	22.05	75.9	19.23	83.91	30.37		
Classification No. 6							
PA (%)	57.55	67.58	18.06	78.66	57.81	55.37	0.5322
UA (%)	55.04	72.55	21.23	73.84	51.41		
Classification No. 7							
PA (%)	58.38	51.43	12.05	76.25	65.99	51.06	0.4719
UA (%)	51.31	58.45	17.69	64.37	54.70		
Classification No. 8							
PA (%)	**92.57**	**89.25**	**89.00**	**86.13**	**88.37**	**88.72**	**0.8615**
UA (%)	**90.00**	**82.00**	**88.00**	**90.15**	**91.75**		

PA, Producer's accuracy (%); UA, User's accuracy (%); OA, Overall accuracy (%)

PAN significantly increased the overall accuracy of all the classes including urban and water bodies as evident from Table 7 and Table 8 (highlighted in bold). There was a 7.6% increase in accuracy by adding temperature, NDVI, EVI, elevation, slope, aspect, PAN along with texture measures, which proved to be useful for medium spatial resolution data such as ETM+ while discriminating different classes in an urban environment.

Forested Landscape with Undulating Terrain Classification: Uttara Kannada, Central Western Ghats

Figure 4 shows output from the seven classified images and the LU statistics are listed in Table 9. The producer's, user's and overall accuracies with kappa are given in Table 10. Inclusion of NDVI in spectral bands classification produced very low accuracy, so was removed from further analysis. Figure 4 shows that addition of elevation, slope and aspect did not improve classification accuracy (Classification No. 3 and 5), and hence were removed from subsequent classifications. Addition of these layers misclassified forest as plantation (>40% of the area was misclassified as plantation) and wasteland were under estimated. Water bodies could not be detected.

Outputs obtained from original spectral bands along with temperature, EVI and PAN (Classification No. 2, 4 and 6) have improved classification results. Texture could not resolve differences between plantation and forest, and plantation was under estimated in classification. From Table 10, it is evident that temperature plays a major role in classification in a forested area which had highest classification accuracy (Classification No. 2 with 88.26% overall accuracy highlighted in bold in Table 10). EVI increased the classification accuracy by 4.3% (Classification No. 4) and temperature, EVI and PAN together increased the overall accuracy by 1.6% (in Classification No. 6) compared to the classification of only original spectral bands. All other layer combinations decreased the accuracy. Overall, the highest classification

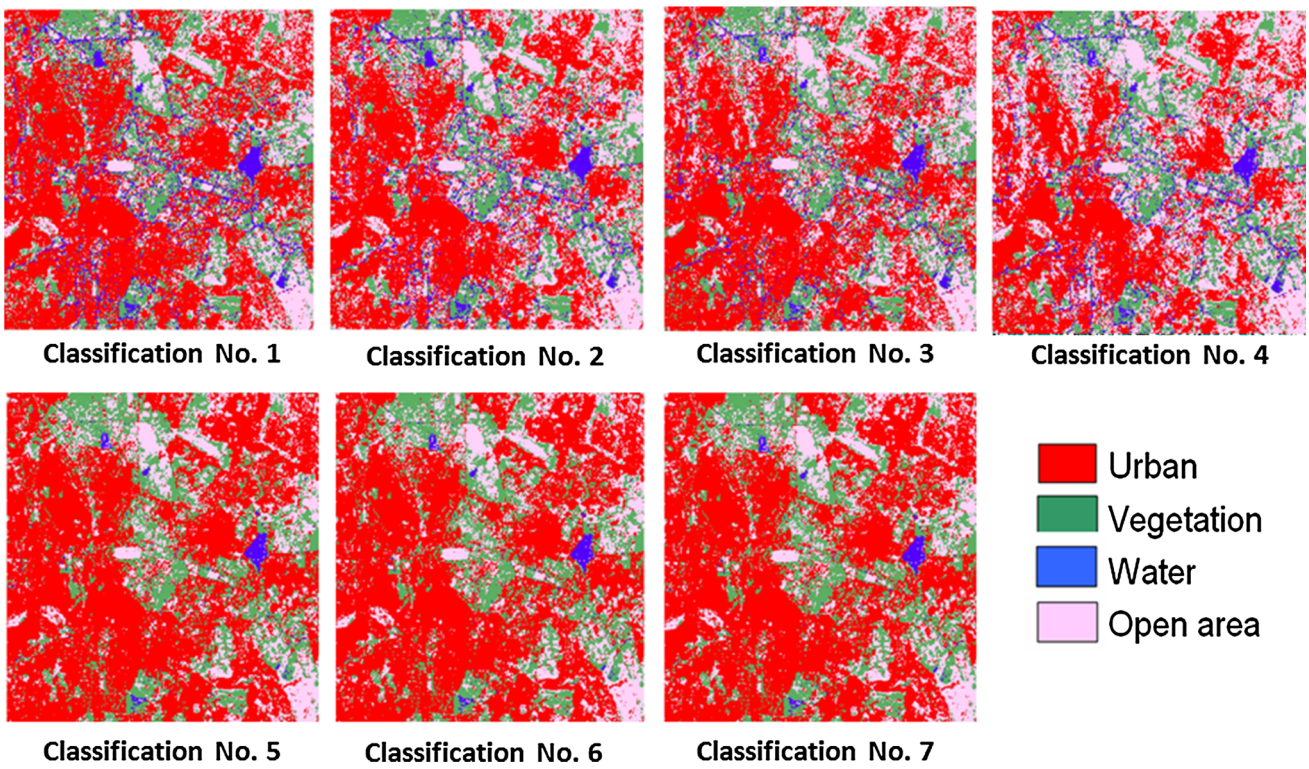

Fig. 3 Classified outputs from Landsat ETM+ bands by adding additional geographical layers (colour figure online)

Table 7 Area statistics obtained from the Landsat ETM+ classified images for Bangalore City

Area		Class				
		Urban	Vegetation	Water	Open area	Total
Classification 1	ha	4543.14	1911.89	600.32	1999.25	9054.62 ha
	%	50.17	21.12	6.63	22.08	(100%)
Classification 2	ha	4014.78	1825.96	560.71	2653.15	
	%	44.34	20.17	6.19	29.30	
Classification 3	ha	4245.71	1884.53	471.43	2446.04	
	%	46.93	20.83	5.21	27.03	
Classification 4	ha	3450.37	1854.25	554.54	3188.55	
	%	38.14	20.49	6.13	35.24	
Classification 5	ha	**5262.71**	**1905.61**	**93.96**	**1754.99**	
	%	**58.36**	**21.13**	**1.04**	**19.46**	
Classification 6	ha	**5226.04**	**1887.87**	**86.47**	**1816.89**	
	%	**57.96**	**20.94**	**0.96**	**20.15**	
Classification 7	ha	**5164.41**	**1974.06**	**65.70**	**1813.11**	
	%	**57.27**	**21.89**	**0.73**	**20.11**	

accuracy improved by 6.7% with temperature as an additional layer.

Mountainous Terrain: Mandhala Watershed, Western Himalaya

Figure 5 shows output from the nine classified images, LC statistics are listed in Table 11 and accuracy assessment is given in Table 12. Figure 5 shows that classification of only 6 spectral bands and addition of EVI (Classification No. 1 and 4) have over estimated the "others" category.

In Classification No. 8 (ETM+ bands 1, 2, 3, 4, 5, 7 with temperature, EVI and texture) and Classification No. 9 (ETM+ bands 1, 2, 3, 4, 5, 7 and texture), others category was not identified. In both these cases, vegetation was over estimated because of misclassification of others category.

Table 8 Accuracy assessment of the Landsat ETM+ classified images for Bangalore City

Accuracy	Class					
	Urban	Vegetation	Water	Open area	OA (%)	Kappa
Classification No. 1						
PA (%)	73.94	87.45	66.91	74.62	75.50	0.7309
UA (%)	76.92	84.36	61.00	78.82		
Classification No. 2						
PA (%)	76.22	87.99	68.62	79.52	77.94	0.7548
UA (%)	78.73	83.05	65.28	81.03		
Classification No. 3						
PA (%)	71.88	78.87	69.96	71.09	73.12	0.7101
UA (%)	74.70	77.95	65.23	75.29		
Classification No. 4						
PA (%)	68.33	81.87	57.34	77.11	71.43	0.6811
UA (%)	75.19	78.33	59.61	72.55		
Classification No. 5						
PA (%)	**83.57**	**82.41**	**78.91**	**81.88**	**81.84**	**0.7978**
UA (%)	**83.64**	**83.37**	**80.85**	**81.76**		
Classification No. 6						
PA (%)	**83.99**	**82.59**	**79.15**	**82.13**	**82.29**	**0.8077**
UA (%)	**83.94**	**83.77**	**81.17**	**82.44**		
Classification No. 7						
PA (%)	**84.91**	**88.21**	**81.11**	**83.62**	**83.15**	**0.8125**
UA (%)	**81.17**	**81.57**	**84.23**	**80.51**		

PA, Producer's accuracy (%); UA, User's accuracy (%); OA, Overall accuracy (%)

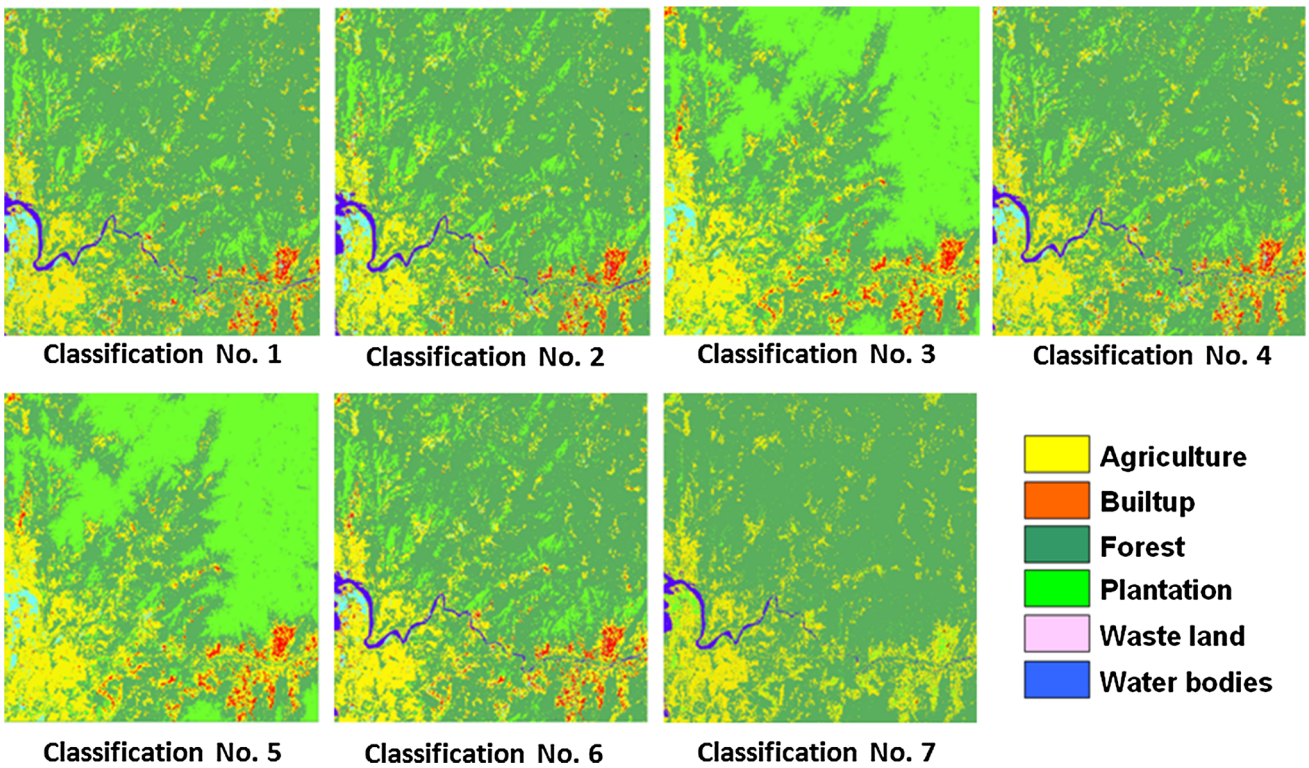

Fig. 4 Classified outputs of Landsat ETM+ bands by adding additional geographical layers from a part of Central Western Ghats (colour figure online)

Table 9 Area statistics obtained from the Landsat ETM+ classified images (part of Central Western Ghats)

Area		Class					
		Agriculture	Builtup	Forest	Plantation	Wasteland	Water
Classification 1	ha	8721.71	730.03	37671.87	4197.55	885.99	651.34
	%	16.5	1.38	71.26	7.94	1.68	1.23
Classification 2	ha	8179.03	853.60	36978.03	5194.64	929.38	723.79
	%	15.47	1.61	69.96	9.83	1.76	1.37
Classification 3	ha	9314.73	889.17	20812.48	21359.72	482.38	–
	%	17.62	1.68	39.37	40.41	0.91	–
Classification 4	ha	8973.28	709.15	37594.65	4058.98	898.02	624.40
	%	16.98	1.34	71.12	7.68	1.70	1.18
Classification 5	ha	9737.47	851.73	19589.41	22217.03	462.84	–
	%	18.42	1.61	37.06	42.03	0.88	–
Classification 6	ha	9455.82	892.81	36491.99	4745.47	604.38	666.02
	%	17.89	1.69	69.04	8.98	1.14	1.26
Classification 7	ha	8558.35	8.50	42688.61	276.25	822.53	504.24
	%	16.19	0.02	80.76	0.52	1.56	0.95
Total	ha	52858.47					

Table 10 Accuracy assessment of the Landsat ETM+ classified images from a part of Central Western Ghats

Accuracy	Class							
	Agriculture	Builtup	Forest	Plantation	Wasteland	Water	OA	Kappa
Classification No. 1								
PA	74.36	81.15	79.55	81.00	78.72	81.88	81.56	0.7856
UA	86.67	83.85	77.80	84.62	80.00	82.59		
Classification No. 2								
PA	92.86	88.15	87.20	85.66	88.72	89.56	**88.26**	**0.8643**
UA	86.67	88.15	89.66	86.92	87.00	89.44		
Classification No. 3								
PA	61.76	68.18	61.90	53.85	55.22	–	61.59	0.4931
UA	66.67	59.22	65.14	62.31	57.48	–		
Classification No. 4								
PA	78.74	88.15	83.78	80.09	88.72	85.55	**85.87**	**0.8326**
UA	96.67	88.15	81.23	82.31	81.11	87.23		
Classification No. 5								
PA	61.84	68.19	61.81	59.49	65.19	–	61.69	0.4874
UA	63.34	60.33	55.59	60.31	60.65	–		
Classification No. 6								
PA	83.34	81.91	77.38	79.91	85.28	88.01	**83.16**	**0.8014**
UA	85.55	82.48	81.68	82.30	83.77	86.34		
Classification No. 7								
PA	84.55	71.88	74.88	–	72.00	81.00	77.64	0.7552
UA	80.73	62.96	78.02	–	83.51	88.58		

PA, Producer's accuracy (%); UA, User's accuracy (%); OA, Overall accuracy (%)

The optimum LC classification result with different layers is highlighted in bold in Table 11 (Classification No. 7). From accuracy assessment (Table 12), it is evident that addition of each layer in subsequent classifications improvised the classification accuracy (Classification No. 2–7), compared to only spectral bands (Classification No. 1). Output obtained from original spectral bands along with temperature, EVI, elevation, slope, aspect and PAN showed highest classification accuracy. However, addition of texture did not show any improvement in classification

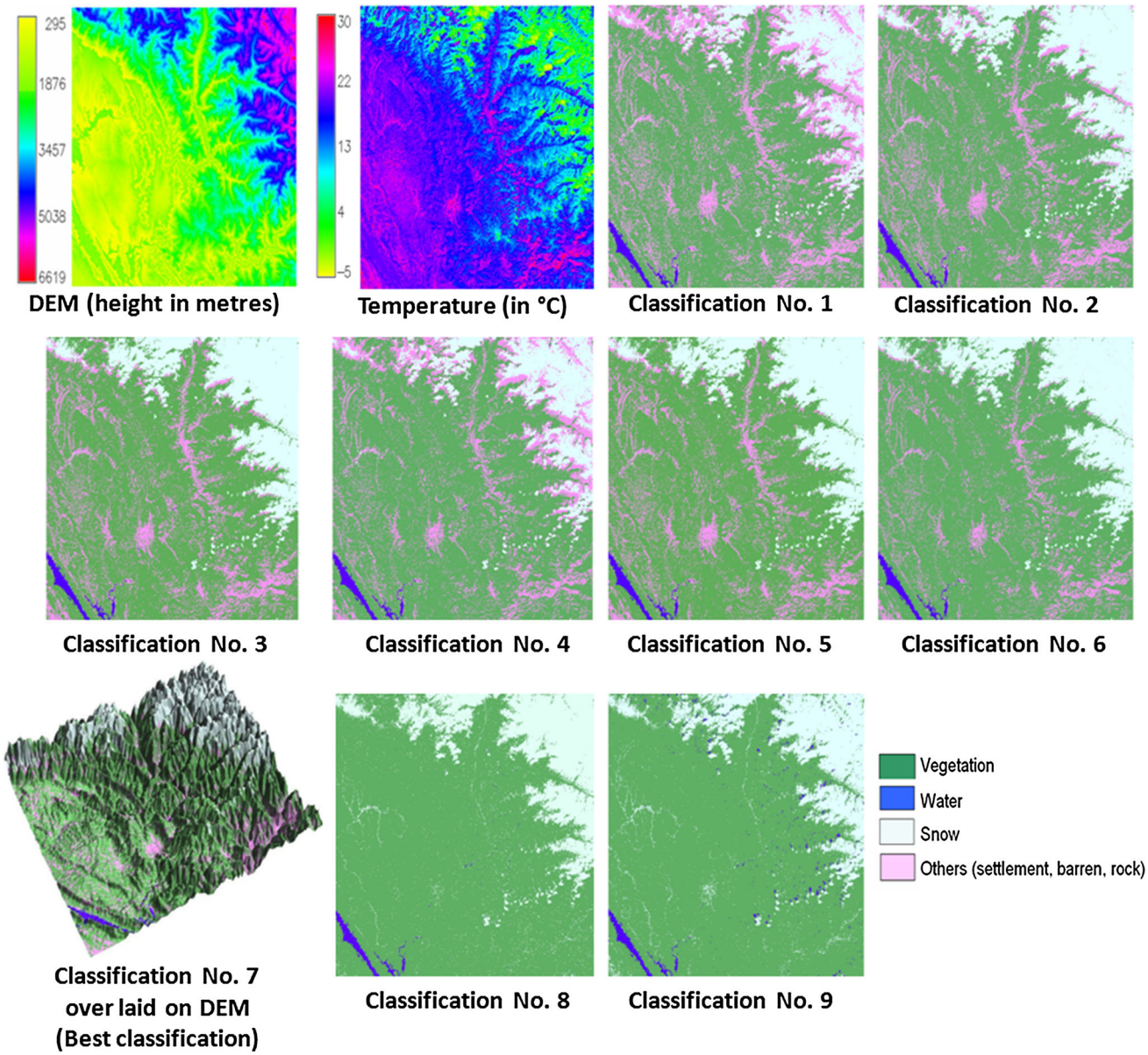

Fig. 5 Classified outputs from Landsat ETM+ bands by adding additional geographical layers (part of Western Himalaya) (colour figure online)

(Classification No. 8 and 9). Addition of temperature layer increased the classification accuracy by 3.76% (Classification No. 2), elevation by 4.18% (Classification No. 3), EVI by 1% (Classification No. 4), elevation, slope and aspect by 5.32% (Classification No. 5) and temperature, EVI, elevation, slope, aspect and PAN together increased the overall accuracy by 10.84% (in Classification No. 7) compared to the classification of only original spectral bands. From Table 12, it is evident that in a rugged terrain with temperate climate, temperature, EVI, elevation, slope, aspect and PAN play major role in improving the classification with highest accuracy (89.97% in Classification No. 7 highlighted in bold in Table 12). However, texture combinations decreased the accuracy.

In this work, derived and ancillary layers were assessed for their performance in improving classification accuracy in three different terrains such as urbanised landscape, forested landscape with undulation and rugged terrain with temperate climate. The results provided new insights to the likelihood of improved performance of LC classification by use of supplemental layers related to the region along with the RS data. IKONOS data were used only for urban area classification along with many other layers of elevation and texture. The enhanced characteristics of IKONOS MS and PAN compared to Landsat ETM+ or IRS LISS-III highlighted some typical urban features such as buildings and narrow roads in residential areas compared to the latter (Fig. 2, 3). IKONOS image

Table 11 Area statistics obtained from the Landsat ETM+ classified images of Western Himalaya

Area		Class			
		Vegetation	Water	Snow	Others (settlement, barren, rock)
Classification 1	ha	916357	12,725	168,825	352,291
	%	63.19	0.88	11.64	24.29
Classification 2	ha	940,477	12,538	248,346	248,838
	%	64.85	0.86	17.12	17.16
Classification 3	ha	939,836	12,410	269,573	228,379
	%	64.81	0.86	18.52	15.75
Classification 4	ha	984,622	12,677	176,550	276,350
	%	67.90	0.87	12.17	19.06
Classification 5	ha	962,457	12,484	276,213	199,044
	%	66.37	0.86	19.05	13.73
Classification 6	ha	1,008,109	12,441	280,383	149,265
	%	69.52	0.86	19.33	10.29
Classification 7	ha	**1,009,705**	**12,423**	**279,577**	**148,493**
	%	**69.63**	**0.86**	**19.28**	**10.24**
Classification 8	ha	1,156,003	11,202	282,994	–
	%	79.71	0.77	19.51	–
Classification 9	ha	1,172,211	20,207	257,781	–
	%	80.83	1.39	17.78	–
Total	ha	1,450,198			
	%	100			

not only reduced the mixed pixel problem, but also provided a rich texture and contextual information than Landsat ETM+ MS bands with 15 or 30 m spatial resolution. Earlier works (Gong et al. 1992; Shaban and Dikshit 2002) have used SPOT HRV data for urban classification due to its high spatial resolution comparing with Landsat ETM data. Knowledge based expert system have also been used with MS imagery and LiDAR data to delineate impervious surface in urban areas (Germaine and Hung 2011). The study confirmed that high spatial resolution is considered to be more important than high spectral resolution in urban classification (Jensen and Cowen 1999). In IKONOS data classification, when only DEM and texture measures were added as input to the classifier apart from IKONOS 4 spectral bands, the overall accuracy went high to 88.72% (3.5% improvement) with high producer's and user's accuracies for individual classes, which is comparable to the overall accuracy obtained by classifying QuickBird imagery for LC classification in a complex urban environment based on texture (overall accuracy—87.33%) and segmentation (overall accuracy—88.33%) by Lu et al. (2010). Although it is difficult to identify suitable texture which is dependent on image band and window size for the specific study (Chen et al. 2004), appropriate texture measures reduce spectral variation within same LC and also improves spectral separability among different LC classes (Augera et al. 2008; Lu et al. 2008a, b). It is to be noted that derived layers from elevation such as slope and aspect did not aid in discriminating classes and EVI did not prove useful in classification due to poor vegetation cover in the urban area. Addition of temperature, NDVI, EVI, elevation, slope, aspect, PAN and texture layers with Landsat ETM+ spectral bands 1, 2, 3, 4, 5 and 7, significantly improved the classification accuracy by 7.6%, which proved to be useful with medium spatial resolution data in an urban area.

In a forested terrain, temperature played major role in classification, producing highest classification accuracy (88.26%), which is an improvement of 6.7% compared to the classification of only spectral bands. Because of various complex surface features, hilly regions are difficult to classify using RS data. In a rugged terrain with temperate climate and high altitudinal variations, inclusion of temperature, EVI, elevation, slope, aspect and PAN layers played a major role in increasing the classification accuracy to 89.97% (improvement by 10.84%), compared to the classification of only original spectral bands. This accuracy is higher than use of fractal dimension data and original ETM+ data in a Chinese subtropical hilly region (accuracy of 80.69%) by Zhu et al. (2011). Individually, the maximum increase in overall accuracy was noticed by the addition of slope and aspect to the original spectral bands (improvement in classification accuracy by 5.32%).

Table 12 Accuracy assessment of the Landsat ETM+ classified images (Western Himalaya)

Accuracy	Class					
	Vegetation	Water	Snow	Others	OA	Kappa
Classification No. 1						
PA	71.78	88.11	86.00	71.00	79.13	0.7789
UA	73.13	85.98	84.00	73.00		
Classification No. 2						
PA	79.78	89.09	87.22	75.29	82.98	0.7999
UA	81.02	85.98	85.09	78.31		
Classification No. 3						
PA	79.46	88.78	83.29	79.85	83.31	0.8122
UA	82.45	89.36	85.90	77.06		
Classification No. 4						
PA	79.78	81.09	80.98	79.03	80.18	0.7865
UA	78.21	82.98	82.45	77.10		
Classification No. 5						
PA	83.33	87.93	84.49	85.29	84.45	0.8222
UA	85.00	88.17	80.22	83.30		
Classification No. 6						
PA	85.06	88.20	85.21	86.91	87.23	0.8511
UA	87.25	89.90	87.35	88.22		
Classification No. 7						
PA	**89.11**	**90.01**	**88.58**	**89.27**	**89.97**	**0.8755**
UA	**88.15**	**92.90**	**90.70**	**91.01**		
Classification No. 8						
PA	76.89	80.00	79.28	–	78. 91	0.7581
UA	78.50	77.28	81.51	–		
Classification No. 9						
PA	70.18	80.57	77.04	–	77.19	0.7441
UA	79.50	76.70	79.17	–		

PA, Producer's accuracy (%); UA, User's accuracy (%); OA, Overall accuracy (%)

However, in addition to the use of ancillary layers such as textural images, selection of different seasonal images are also needed to improve classification performance (Lu et al. 2010; Masocha and Skidmore 2011). Selection of a particular set of derived geographical input data along with the original spectral bands for LC classification is generally subjective or random without much insightful consideration, and in most cases ancillary layers are used without the knowledge of their meaningful impact on the final classification result. The present study showed that different combination of the input data can lead to different separation of classes in the feature space. Different classification algorithms can also lead to different compartmentation of the feature space with respect to the classes and both choices can affect the final classification result. In such cases, discussing the aspect of individual derived geographical layers is meaningful. Further, future analysis will focus on the effect and role of ancillary and derived geographical layers in improving the classification accuracy along with new methods of expert classification being developed.

Conclusions

RS based LC mapping and monitoring of large areas has created a new challenge with the varied spatial scale and data volume, requiring automated classification algorithms that minimise human interventions. This work has shown that use of spatial information along with complimentary ancillary and derived geographical layers is an effective way to improve LC classification performance which was demonstrated in three different terrains. In a highly urbanised area with less vegetation cover and highly contrasting features, texture played a major role in discriminating individual classes which were rather difficult to distinguish using only original high spatial resolution IKONOS MS bands. DEM played a role when the terrain is undulating, however, due to limited vegetation cover, vegetation index was not useful in classification. For the same urban area, inclusion of temperature, NDVI, EVI, elevation, slope, aspect, PAN and texture layers significantly increased the overall accuracy by 7.6% while discriminating different classes properly with Landsat ETM+ data. In a forested landscape with moderate elevation, temperature was the only factor that increased the LC classification accuracy. In a rugged terrain with temperate climate, addition of temperature, EVI, elevation, slope, aspect and PAN layers significantly improved the classification accuracy compared to the classification of only original spectral bands. Sometimes, improvements in spatial resolution of the data by integration of the spectral and spatial details from Multispectral and Panchromatic bands through image fusion also helps in object recognition, delineation and improves classification accuracy.

Acknowledgement We are grateful to (1) the NRDMS division, The Ministry of Science and Technology (DST), Government of India, (2) The Ministry of Environment, Forests and Climate Change, Government of India and (3) Indian Institute of Science for the financial and infrastructure support.

References

Augera, F., Aguilar, F. J., & Aguilar, M. A. (2008). Using texture analysis to improve per-pixel classification of very high resolution images for mapping plastic greenhouses. *ISPRS Journal of Photogrammetry and Remote Sensing, 63,* 635–646.

Breiman, L., & Cutler, A. (2010). Breiman and Cutler's random forests for classification and regression. Version 4.5-36, Repository—CRAN. http://ugrad.stat.ubc.ca/R/library/randomForest/html/00Index.html.

Chen, D., Stow, D. A., & Gong, P. (2004). Examining the effect of spatial resolution and texture window size on classification accuracy: An urban environment case. *International Journal of Remote Sensing, 25,* 2177–2192.

Collins, W. J., Bellouin, N., Doutriaux-Boucher, M., Gedney, N., Halloran, P., Hinton, T., Hughes, J., Jones, C. D., Joshi, M., Liddicoat, S., Martin, G., O'Connor, F., Rae, J., Senior, C., Sitch, S., Totterdell, I., Wiltshire, A., & Woodward, S. (2011). Development and evaluation of an Earth-system model—HadGEM2. *Geoscientific Model Development Discussion, 4,* 997–1062.

Dópido, I., Villa, A., Plaza, A., & Gamba, P. (2011). A quantitative and comparative assessment of unmixing-based feature extraction techniques for hyperspectral image classification. *IEEE Journal of Selected Topics in Applied Earth Observations and Remote Sensing*. doi:10.1109/JSTARS.2011.2176721.

Dorren, L. K. A., Maier, B., & Seijmonsbergen, A. C. (2003). Improved Landsat-based forest mapping in steep mountainous terrain using object-based classification. *Forest Ecology and Management, 183*(2003), 31–46.

Fahsi, A., Tsegaye, T., Tadesse, W., & Coleman, T. (2000). Incorporation of digital elevation models with Landsat-TM data to improve land cover classification accuracy. *Forest Ecology and Management, 128*(2000), 57–64.

Germaine, K. A., & Hung, M.-C. (2011). Delineation of impervious surface from multispectral imagery and lidar incorporating knowlwdge based expert system rules. *Photogrammetric Engineering and Remote Sensing, 77*(1), 75–85.

Gong, P., Marceau, D. J., & Howarth, P. J. (1992). A comparison of spatial feature extraction algorithms for land-use classification with SPOT HRV data. *Remote Sensing of Environment, 40,* 137–151.

GRASS GIS. (2017). r.texture, https://grass.osgeo.org/grass72/manuals/r.texture.html.

Haack, B. N., Solomon, E. K., Bechdol, M. A., & Herold, N. D. (2002). Radar and optical data comparison/integration for urban delineation: A case study. *Photogrammetric Engineering and Remote Sensing, 68,* 1289–1296.

Haralick, R. (1979). Statistical and structural approaches to texture. *Proceedings of the IEEE, 67*(5), 786–804. doi:10.1109/PROC.1979.11328.

Haralick, R. M., Shanmugam, K., & Dinstein, I. (1973). Textural features for image classification. *IEEE Transactions on Systems, Man, and Cybernetics, SMC-3*(6), 610–621.

Hostert, P., Roder, A., & Hill, J. (2003). Coupling spectral unmixing and trend analysis for monitoring of long-term vegetation dynamics in Mediterranean rangelands. *Remote Sensing of Environment, 87,* 183–197.

Huang, C., Song, K., Kim, S., Townshend, J. R. G., Davis, P., Masek, J. G., & Goward, S. N. (2008). Use of dark object concept and support vector machines to automate forest cover change analysis. *Remote Sensing of Environment, 112*(2008), 970–985.

Hung, M., & Ridd, M. K. (2002). A subpixel classifier for urban land-cover mapping based on a maximum-likelihood approach and expert system rules. *Photogrammetric Engineering and Remote Sensing, 68,* 1173–1180.

Jensen, J. R., & Cowen, D. C. (1999). Remote sensing of urban/suburban infrastructure and socioeconomic attributes. *Photogrammetric Engineering and Remote Sensing, 65,* 611–622.

Lu, D., Batistella, M., & Moran, E. (2008a). Integration of Landsat TM and SPOT HRG images for vegetation change detection in the Brazilian Amazon. *Photogrammetric Engineering and Remote Sensing, 74*(4), 421–430.

Lu, D., Batistella, M., Moran, E., & de Miranda, E. E. (2008b). A comparative study of Landsat TM and SPOT HRG images for vegetation classification in the Brazilian Amazon. *Photogrammetric Engineering and Remote Sensing, 70*(3), 311–321.

Lu, D., Hetrick, S., & Moran, E. (2010). Land cover classification in a complex urban–rural landscape with Quickbird imagery. *Photogrammetric Engineering and Remote Sensing, 76*(10), 1159–1168.

Lu, D., & Weng, Q. (2005). Urban classification using full spectral information of Landsat ETM+ imagery in Marion County, Indiana. *Photogrammetric Engineering and Remote Sensing, 71*(11), 1275–1284.

Lu, D., & Weng, Q. (2007). A survey of image classification methods and techniques for improving classification performances. *International Journal of Remote Sensing, 28*(5), 823–870.

Masocha, M., & Skidmore, A. K. (2011). Integrating conventional classifiers with a GIS expert system to increase the accuracy of invasive species mapping. *International Journal of Applied Earth Observation and Geoinformation, 13,* 487–494.

Na, X., Zhang, S., Li, Xiaofeng, Yu, H., & Liu, C. (2010). Improved land cover mapping using random forests combined with Landsat Thematic Mapper imagery and ancillary geographic data. *Photogrammetric Engineering and Remote Sensing, 76*(7), 833–840.

Nemani, R., Votava, P., Michaelis, A., Metlon, M., & Milesi, C. (2011). Collaborative supercomputing for global change science. *Eos, 92*(13), 109–116.

Pacheco, A., & McNairn, H. (2010). Evaluating multispectral remote sensing and spectral unmixing analysis for crop residue mapping. *Remote Sensing of Environment, 114,* 2219–2228.

Pu, R., Gong, P., Michishita, R., & Sasagawa, T. (2008). Spectral mixture analysis for mapping abundance of urban surface components from the Terra/ASTER data. *Remote Sensing of Environment, 112,* 939–954.

Ramachandra, T. V., & Kumar, U. (2008). Wetlands of greater Bangalore, India: Automatic delineation through pattern classifiers. *The Greendisk Environmental Journal, (International Electronic Journal), 1*(26), 1–22.

Ramachandra, T. V., & Kumar, U. (2009). Land surface temperature with land cover dynamics: Multi-resolution, spatio-temporal data analysis of Greater Bangalore. *International Journal of Geoinformatics, 5*(3), 43–53.

Recio, J. A., Hermosilla, L. A., & Fernandez-Sarria, A. (2011). Historical land use as a feature for image classification. *Photogrammetric Engineering and Remote Sensing, 77*(4), 377–387.

Shaban, M. A., & Dikshit, O. (2001). Improvement of classification in urban areas by the use of textural features: The case study of Lucknow city, Uttar Pradesh. *International Journal of Remote Sensing, 22,* 565–593.

Shaban, M. A., & Dikshit, O. (2002). Evaluation of the merging of SPOT multispectral and panchromatic data for classification of an urban environment. *International Journal of Remote Sensing, 23,* 249–262.

Smith, M. O., Johnson, P. E., & Adams, J. B. (1985). Quantitative determination of mineral types and abundances from reflectance spectra using principal component analysis. In *Proceedings of the Lunar and Planetary Science Conference*, 90, (pp. 797–904).

Stuckens, J., Coppin, P. R., & Bauer, M. E. (2000). Integrating contextual information with per-pixel classification for improved land cover classification. *Remote Sensing of Environment, 71,* 282–296.

Turner, B. L., II, Meyer, W. B., & Skole, D. L. (1994). Global land-use/land-cover change: Towards and integrated study. *Ambio, Integrating Earth System Science, 23*(1), 91–95.

Xian, G., Crane, M., & McMahon, C. (2008). Quantifying multi-temporal urban development characteristics in Las Vegas from

Landsat and ASTER data. *Photogrammetric Engineering and Remote Sensing, 74*(4), 473–481.

Xiaodong, Na, Shuqing, Z., Huaiqing, Z., Xiaofeng, L., & Chunyue, L. (2009). Integrating TM and ancillary geographical data with classification trees for land cover classification of marsh area. *Chinese Geographical Science, 19*(2), 177–185.

Zhu, J., Shi, J., Chu, H., Hu, J., Li, X., & Li, W. (2011). Remote sensing classification using fractal dimension over a subtropical hilly region. *Photogrammetric Engineering and Remote Sensing, 77*(1), 65–74.